IEEE Access
Multidisciplinary ⋮ Rapid Review ⋮ Open Access Journal

Received 22 October 2022, accepted 15 December 2022, date of publication 2 January 2023, date of current version 10 January 2023.

Digital Object Identifier 10.1109/ACCESS.2022.3233633

RESEARCH ARTICLE

Fast QC Relaxation of the Optimal Power Flow Using the Line-Wise Model for Representing Meshed Transmission Networks

ABDEL RAHMAN ALDIK, (Member, IEEE), AND BALA VENKATESH, (Senior Member, IEEE)
Department of Electrical Engineering, Toronto Metropolitan University, Toronto, ON M5B 2K3, Canada
Centre of Urban Energy, Toronto Metropolitan University, Toronto, ON M5B 2K3, Canada

Corresponding author: Bala Venkatesh (bala@torontomu.ca)

This work was supported in part by the Natural Sciences and Engineering Research Council of Canada (NSERC), and in part by the Mathematics of Information Technology and Complex Systems (MITACS).

ABSTRACT In this paper, we investigate the recently introduced McCormick-based Quadratic Convex (QC) relaxation of the Optimal Power Flow (OPF) where Line-Wise Model (LWM) is used for representing meshed transmission systems (QC-LW OPF) for the sake of decisively determining its relationship to other available convex relaxations in the literature. We also extend the recently introduced convex envelope of the tangent function so it would be suitable for test cases with any voltage angle difference range. A computational study where the recently proposed QC-LW OPF formulation is compared to an equivalent McCormick based QC relaxation of the OPF where Bus Injection Model (BIM) is used for representing meshed transmission systems (QC-BI OPF) is presented in this paper. This computational study was conducted using test cases that belong to different operational categories using 123 test cases from the PGLib-OPF library with a bus size range between 3 up to 6515 buses for the sake of understanding the effect of the change of operating conditions on the quality of solutions obtained using the QC-LW OPF and QC-BI OPF formulations. Results are compared using several metrics that testify to the obtained solution's quality and the problem's computational complexity. Comparison of results shows that the QC-LW relaxation neither dominates nor is dominated by the QC-BI relaxation in terms of solution quality. Therefore, it dominates the Second Order Cone (SOC) relaxation and neither dominates nor is dominated by the Semidefinite Programming (SDP) relaxation. Furthermore, it is shown that the QC-LW OPF has reduced the number of relaxed trigonometric functions and McCormick envelopes needed when compared to the QC-BI OPF, leading to a faster solution time for more than 84% of the test cases in the range of 2% up to 67%.

INDEX TERMS Optimal power flow, convex optimization, convex relaxations, QC relaxation, optimality gap.

NOMENCLATURE

NB	Number of buses.
NG	Number of designated generator buses.
NT	Total number of transmission branches.
$C2_i$, $C1_i$, $C0_i$	Cost coefficients of generator i.
PG_i, QG_i	Active and reactive power generation at bus i.
PD_i, QD_i	Active and reactive power demand at bus i.
U_i	Bus i's squared voltage magnitude.
V_i	Bus i's voltage magnitude.
δ_i	Bus i's voltage angle.
δ_{ab}	Buses a and b 's voltage angle difference.
PF_l, QF_l, PS_l, QS_l	Branch $l's$ active and reactive power flowing into first and second ends (Contributions from shunt elements are not included).
SF_l, SS_l	Branch $l's$ apparent power flowing into first and second ends (Contributions from shunt elements are not included).
Sfm_l, Sto_l	Branch l's apparent power flowing from first to second end and vice versa.

The associate editor coordinating the review of this manuscript and approving it for publication was Ehab Elsayed Elattar.

R_l	Branch l's resistance.
X_l	Branch l's reactance.
Z_l	Branch l's impedance magnitude.
GS_i, BS_i	Total sum of conductance and susceptance shunt elements connected to Bus i.
$G_{al}, G_{bl}, B_{al}, B_{bl}$	Pi-model's conductance and susceptance shunt elements connected to branch $l's$ buses.
$\underline{U_i}, \overline{U}_i$	Bus $i's$ voltage squared magnitude minimum and maximum limits.
$\underline{\delta_l}, \overline{\delta}_l$	Branch $l's$ voltage angle difference minimum and maximum limits.
$\underline{PG_i}, \overline{PG_i}$	Generator $i's$ active power generation minimum and maximum limits.
$\underline{QG_i}, \overline{QG_i}$	Generator $i's$ reactive power generation minimum and maximum limits.
$\overline{SL_l}$	Branch $l's$ maximum limit for apparent power flow.
$TS1_l, TS2_l$	Slopes of the lines that approximate the tangent function.
TSM_l	Slope of the line that connects the points $(\underline{\delta_l}, \tan(\underline{\delta_l}))$ and $(\overline{\delta}_l, \tan(\overline{\delta}_l))$.
TC_l	Tangent function's convex envelope.
$\beta 1_l, \beta 2_l$	Offset values needed for defining the lines that bound the convex envelope of the tangent function.
$\delta 1_{Tl}, \delta 2_{Tl}$	Angles at which lines can be drawn to be tangential to the tangent function to form a convex envelope of it.
E_l	Auxiliary variables that is equivalent to the expression $V_a \cdot V_b \cdot \cos(\delta_{ab})$.
W_l	Auxiliary variable to express the McCormick envelope of the expression $K_l \cdot TC_l$.
Ω	Set of summation limits for calculating $CNCV$ for each of the state variables in the set γ.

I. INTRODUCTION

OPTIMAL power flow (OPF) is a nonconvex power system optimization problem that aims to minimize the total generation cost while taking operational constraints into account [1]. Its importance comes from the fact that since it was formulated in 1962 [2], it remains a fascinating technical challenge. This can be attributed to the problem of nonconvexity that obstructs the ability of solving it efficiently to global optimality. Such a shortcoming has direct economic consequences. The Federal Energy Regulatory Commission (FERC) estimates that about 400 billion dollars is left untapped worldwide if the optimality gap between global solutions of the OPF and currently obtained solutions is assumed to be 10% [3].

A. LITERATURE SURVEY- CONVENTIONAL OPF FORMULATIONS

The nonconvexity of the OPF problem has been illustrated by studying the feasible space of several small test cases in [4]. Several approaches for solving the OPF problem have been discussed in the literature. These approaches include applying the gradient method to provide a feasible solution for the OPF problem [5], [6], the use of quadratic programming [7], [8], [9], the use of heuristic optimization techniques [10], [11] as well as the use of approximated convex models for solving the OPF problem [12], [13], [14], [15]. The use of nonlinear solvers that provide local solutions was also investigated in the literature [16], [17], [18]. However, all these mentioned techniques suffer from one of two major drawbacks. Namely, they suffer from the drawback of either the inability of finding a global solution for the OPF or finding a global solution for the approximated problem that is not feasible for the original nonconvex OPF problem.

B. LITERATURE SURVEY- CONVEX OPF FORMULATIONS

Most recently, the advances in the field of convex conic optimization have encouraged the pursuit of a new approach for solving the OPF problem [19]. Several convex relaxations have been discussed and compared in the literature. The comparisons usually aim to determine how tight a certain convex relaxation technique is and how related the convex relaxation techniques are to each other. Such convex relaxations include Second Order Cone (SOC) [19], Semidefinite Programming (SDP) [20], and Quadratic Convex (QC) relaxations [21]. SOCP relaxation can be exact under certain conditions for radial systems, easy to implement, and efficiently solved where formulations can be created without using bus voltage phasor angles [22], [23], [24]. However, the same cannot be extended to meshed network models where the use of bus voltage phasor angles is a must and thus there is a need for more suitable convex relaxations. SDP relaxation has been shown to provide a tighter relaxation that manages to find a feasible global solution for different test systems [23], [24], [25]. However, it was found that SDP relaxation was not able to find a physically meaningful solution when used for solving the OPF for several practical systems [26]. Moreover, the available solvers are not as efficient as the solvers that can be used for solving Linear Programming (LP) and SOCP formulations, particularly for larger systems and problems that have a mixed integer nature. QC relaxation is reported in the literature to be easier to apply and more computationally efficient as introduced in [21] and [27]. The QC relaxation introduces convex relaxations in the OPF formulation by introducing two novel convex envelopes for the sine and cosine functions and by utilizing McCormick envelopes to create convex envelopes for nonconvex expressions [28]. The importance of McCormick envelopes arises from the fact that the multiplication of two convex envelopes results in another convex envelope, albeit with lower tightness. The QC

relaxation was studied further to increase its tightness by adding more constraints that were inspired by the relationships between power system variables in [29]. The reader is referred to [30] and [31] for more thorough literature about convex relaxations.

Despite the inexactness of convex relaxations that can yield solutions that are not physically meaningful for power system optimization problems, the use of convex relaxations has several advantages [21], [30]. The main advantage is the possibility of finding the global optimum for the original nonconvex problem if the solution of the relaxed formulation is feasible for the original nonconvex problem. In addition, a convex relaxation of a nonconvex formulation can determine a lower or upper bound for the objective function of the nonconvex formulation. Also, they provide a better alternative to existing linear approximation methods that are being used to solve such problems. This is especially true since linear approximations are very sensitive to the change in power system operating point and tend to exhibit poor performance during extreme circumstances that may lead to blackouts [1]. Moreover, it was found that imposing small angle difference bounding constraints could lead to the infeasibility of linear approximation methods for solving the OPF problem [32]. Furthermore, the utilization of convex relaxations for solving power system problems of integer and mixed-integer nature is extremely superior in terms of solution quality and computational efficiency to the use of linear approximation methods [31]. Convex relaxations can also help in identifying infeasibility of power system optimization problems for certain data sets [33]. Furthermore, some convex relaxations have associated sufficient conditions which guarantee their ability to provide global optima for certain limited classes of power system optimization problems [30], [34]. All of these factors justify the growing interest in creating convex relaxations of nonconvex power system problems such as OPF.

C. MOTIVIATION FOR THIS WORK

The Bus Injection Model (BIM) of power balance equations used in [21] is popular and currently the standard formulation for benchmarking efforts that is used by the IEEE PES PGLib-OPF Task Force [33]. However, the existence of other models of power balance equations provides an opportunity to explore the benefits of applying existing convex relaxation techniques or introducing new relaxation techniques that are more suitable. One example of a promising model of power balance equations is the Sparse-Tableau Representation (STR) [35]. The STR model has been relaxed and used for solving the OPF problem where two new relaxations were introduced [36].

Another promising model for power balance equations is the Line-Wise Model (LWM) [37]. This model has shown its superiority in terms of enhancing computational efficiency when compared to the BIM for solving the power flow problem as well as the linearized OPF problem that was solved iteratively using successive linear programming [12], [37], [38], [39]. A special version of the LWM was introduced and convex relaxed for solving the capacitor placement problem in radial distribution systems and was found to significantly reduce solver's computational time [40]. Most recently, a McCormick based QC relaxation of the LWM was introduced as part of an algorithm for solving the Transmission Network Expansion Planning (TNEP) problem in which a novel convex envelope of the tangent function was introduced for test cases where $\left|\underline{\delta}_l\right| = \left|\overline{\delta}_l\right|$ [41]. The proposed formulation was used for solving the OPF problem for 5 test systems with bus size range of 6 up to 118. The reported results in [41] has shown that the McCormick based QC relaxation of the LWM-based OPF formulation (QC-LW OPF) has managed to outperform the McCormick based QC relaxation of the BIM-based OPF formulation (QC-BI OPF) in terms of computational complexity while providing solutions of similar quality for these test cases. Moreover, a novel SDP relaxation of the LW OPF formulation for meshed transmission networks was introduced in the literature recently [42]. Obtained results in [42] have shown its merits in terms of enhancing solution quality and reducing computational complexity for different test cases over the widely used SDP relaxation of the BIM based OPF formulation.

D. PAPER CONTRIBUTIONS

This paper provides a computational study that utilizes the proposed QC-LW OPF formulation in [41] for solving the OPF problem for a wider range of test cases with a larger bus size range and different operational categories. Such computational study is important to decisively establish the relationship between the proposed QC-LW OPF formulation in [41] and the QC-BI OPF that is widely used in the literature in terms of solution's quality and computational complexity. The main contributions of this papers are:

1) The extension of a closed-form novel convex envelope for the tangent function that was introduced in [41] so it would be able to accommodate test cases where $\left|\underline{\delta}_l\right| \neq \left|\overline{\delta}_l\right|$. Such extension is needed in cases where bound tightening of voltage magnitude and angle difference is applied for enhancing the solution quality of convex relaxations [29].
2) The establishment of the relation between the proposed QC-LW OPF formulation [41] and other existing convex relaxations in the literature in terms of solution's quality and computational efficiency. This is done by comparing the QC-LW OPF with the previously introduced QC relaxation of the BIM OPF that was enhanced by adding valid inequalities (QC-BI OPF) [21], [27], [29]. The results of this comparison as well as the already established relationship between the QC-BI OPF and other convex relaxations of the OPF in the literature [21] would be utilized for this manner. The comparison metrics include the Optimality Gap (OG) between the obtained value of the problem's objective function via convex relaxation and the best obtained value of the problem's objective function using a nonconvex solver, the use of the newly

introduced Cumulative Normalized Constraint Violation (*CNCV*) coefficients that were introduced recently to measure the distance to AC feasibility of the obtained solutions by the QC-BI OPF and QC-LW OPF [32] as well as solver's computational time to solve the convex relaxed OPF.

3) The study of the effect of the operating conditions on the quality of the solutions that were obtained by solving the QC-BI OPF and QC-LW OPF formulations for different test cases that belong to three operating conditions.

II. NONCONVEX LW OPF

The most common objective function for the OPF is used where the minimization of active power generation is expressed by (1).

$$Minimize \sum_{i=1}^{NG} \left(C2_i \cdot PG_i^2 + C1_i \cdot PG_i + C0_i \right) \tag{1}$$

Subject to:

The LWM set of equality constraints (2) – (7) that consists of 4 nonconvex constraints that describe the relationship between the bus voltage magnitude, angle, and active and reactive power flow variables (2) – (5) and two linear active and reactive power balance equations (6) – (7). The derivation of the M matrix has been explained in [37]. Other operational constraints for the OPF problem are provided in (8) – (13). It is of great importance to highlight that pi-model was used for modeling both transmission lines and transformers. Hence, all resulting shunt elements are accounted for in (6) – (7) through the parameters GS_i and BS_i and in (12) – (13) through the parameters G_{al}, B_{al}, G_{bl}, B_{bl}. More information about this formulation can be found in [12], [38], [39], [41], and [42].

$$U_a^2 + 2U_a \cdot \left(PF_l \cdot R_l + QF_l \cdot X_l - \frac{U_b}{2} \right) + SF_l^2 \cdot Z_l^2 = 0$$
$$\forall l = 1 \; to \; NT, \quad (a,b) \in l \tag{2}$$

$$U_b^2 + 2U_b \cdot \left(PS_l \cdot R_l + QS_l \cdot X_l - \frac{U_a}{2} \right) + SS_l^2 \cdot Z_l^2 = 0$$
$$\forall l = 1 \; to \; NT, \quad (a,b) \in l \tag{3}$$

$$(PF_l \cdot R_l + QF_l \cdot X_l + U_a) \cdot tan(\delta_{ba}) - PF_l \cdot X_l + QF_l \cdot R_l = 0$$
$$\forall l = 1 \; to \; NT, \quad (a,b) \in l \tag{4}$$

$$(PS_l \cdot R_l + QS_l \cdot X_l + U_b) \cdot tan(\delta_{ab}) - PS_l \cdot X_l + QS_l \cdot R_l = 0 \forall l = 1 \; to \; NT, \quad (a,b) \in l \tag{5}$$

$$[M] \begin{bmatrix} PF \\ PS \end{bmatrix} - U \cdot GS = PD - PG \tag{6}$$

$$[M] \begin{bmatrix} QF \\ QS \end{bmatrix} + U \cdot BS = QD - QG \tag{7}$$

$$\underline{U_i} \le U_i \le \overline{U_i} \quad \forall i = 1 \; to \; NB \tag{8}$$

$$\underline{\delta_l} \le \delta_{ab} \le \overline{\delta_l} \quad \forall l = 1 \; to \; NT, \quad (a,b) \in l \tag{9}$$

$$\underline{PG_i} \le PG_i \le \overline{PG_i} \quad \forall i = 1 \; to \; NG \tag{10}$$

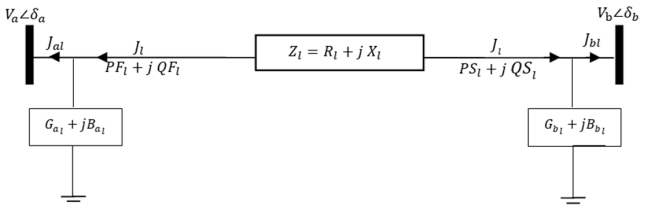

FIGURE 1. The l^{th} branch pi-model. Note that pi-model is used for representing both lines and/or transformers.

$$\underline{QG_i} \le QG_i \le \overline{QG_i} \quad \forall i = 1 \; to \; NG \tag{11}$$

$$(PF_l - U_a \cdot G_{al})^2 + (QF_l + U_a \cdot B_{al})^2 \le \overline{SL_l}^2$$
$$\forall l = 1 \; to \; NT, \quad (a,b) \in l \tag{12}$$

$$(PS_l - U_b \cdot G_{bl})^2 + (QS_l + U_b \cdot B_{bl})^2 \le \overline{SL_l}^2$$
$$\forall l = 1 \; to \; NT, \quad (a,b) \in l \tag{13}$$

We note that the LW OPF depends on the use of the squared voltage U_i and there are no multiplication expressions for the voltage values of buses $V_i \cdot V_j$, which is not the case for the BI OPF formulation that is used to represent power systems in [21], [27], and [33].

III. QC RELAXATION OF THE LW OPF

The McCormick based QC relaxation of the nonconvex LW OPF formulation (1) – (13) is briefly introduced in this section. Full derivation of the QC-LW OPF formulation is provided in [41].

A. CONVEX RELAXATION OF CONSTRAINTS (2) – (3)

The constraints (2) – (3) are replaced by

$$U_a + 2\left(PF_l \cdot R_l + QF_l \cdot X_l - \frac{U_b}{2} \right) + J_l \cdot Z_l^2 = 0$$
$$\forall l = 1 \; to \; NT, \quad (a,b) \in l \tag{14}$$

$$U_b + 2\left(PS_l \cdot R_l + QS_l \cdot X_l - \frac{U_a}{2} \right) + J_l \cdot Z_l^2 = 0$$
$$\forall l = 1 \; to \; NT, \quad (a,b) \in l \tag{15}$$

$$J_l \cdot U_b \ge PS_l^2 + QS_l^2$$
$$\forall l = 1 \; to \; NT, \quad (a,b) \in l \tag{16}$$

B. CONVEX RELAXATION OF CONSTRAINTS (4) – (5)

The constraints (4) – (5) are replaced by

$$W_l - PF_l \cdot X_l + QF_l \cdot R_l = 0, \quad \forall l = 1 \; to \; NT \tag{17}$$

$$-W_l - PS_l \cdot X_l + QS_l \cdot R_l = 0, \quad \forall l = 1 \; to \; NT \tag{18}$$

where W_l is a McCormick envelope that was defined to convexify the expression $E_l \cdot TC_l$ as follows:

$$W_l \ge \underline{E_l} \cdot TC_l + E_l \cdot \underline{TC_l} - \underline{E_l} \cdot \underline{TC_l}$$
$$W_l \ge \overline{E_l} \cdot TC_l + E_l \cdot \overline{TC_l} - \overline{E_l} \cdot \overline{TC_l}$$
$$W_l \le \overline{E_l} \cdot TC_l + E_l \cdot \underline{TC_l} - \overline{E_l} \cdot \underline{TC_l}$$
$$W_l \le \underline{E_l} \cdot TC_l + E_l \cdot \overline{TC_l} - \underline{E_l} \cdot \overline{TC_l}$$
$$\forall l = 1 \; to \; NT \tag{19}$$

E_l is a linear (and thus convex) replacement of the nonconvex expression $V_a \cdot V_b \cdot \cos(\delta_{ab})$ since $V_a \cdot V_b \cdot \cos(\delta_{ab}) = PS_l \cdot R_l + QS_l \cdot X_l + U_b$ [37]:

$$E_l = PS_l \cdot R_l + QS_l \cdot X_l + U_b \quad \forall l = 1 \; to \; NT, \quad (a, b) \in l \tag{20}$$

And TC_l is a convex envelope of the tangent function over a specified voltage angle difference range. Note that in (18), we used a negative sign for W_l since $tan(\delta_{ab}) = -tan(\delta_{ba})$. The derivation of the QC-LW OPF formulation that was illustrated in [41] shows the process for deriving a convex envelope for the tangent function in which $|\underline{\delta_l}| = |\overline{\delta}_l|$. In this paper, we provide a derivation for the tangent function's convex envelope for a more general case where $|\underline{\delta_l}| \neq |\overline{\delta}_l|$. The derivation process depends on studying the nature of the tangent function in the angle range $-\frac{\pi}{2} \leq \delta_{ab} \leq \frac{\pi}{2}$. It has been established that the tangent function is convex for the angle range $0 \leq \delta_{ab} \leq \frac{\pi}{2}$ and concave for the angle range $-\frac{\pi}{2} \leq \delta_{ab} \leq 0$ with $\delta_{ab} = 0$ as the point of inflection where the tangent function transits from being concave to convex and vice versa [43]. This implies that the convex envelope of the tangent function should be studied for three cases depending on the voltage difference angle range as follows:

1) CONVEX ENVELOPE OF THE TANGENT FUNCTION WHERE $\underline{\delta_l} < 0, \overline{\delta}_l > 0$ AND $-\frac{\pi}{2} \leq \delta_{ab} \leq \frac{\pi}{2}$

In the case, the tangent function would not be convex over this angle range. Hence, we need to define two boundary lines that would be tangential to the tangent function to create a convex envelope for it. Starting with $\underline{\delta_l}$, we define a line that approximates the tangent function within the range $-|\underline{\delta_l}| \leq \delta_{ab} \leq |\underline{\delta_l}|$. The slope of the line can be found using the relationship:

$$TS1_l = \frac{tan\left(|\underline{\delta_l}|\right) - tan\left(-|\underline{\delta_l}|\right)}{|\underline{\delta_l}| - -|\underline{\delta_l}|} = \frac{tan\left(|\underline{\delta_l}|\right)}{|\underline{\delta_l}|} \quad \forall l = 1 \; to \; NT \tag{21}$$

Similarly, for $\overline{\delta}_l$, we obtain the slope $TS2_l$ for a line that approximate the tangent function in the range $-|\overline{\delta}_l| \leq \delta_{ab} \leq |\overline{\delta}_l|$. We then use the equations of the linear approximations of the tangent function [$TS1_l \cdot \delta_{ab}$and $TS2_l \cdot \delta_{ab}$] to define two boundary lines that will surround the portion of the function under study as shown in (22).

$$\begin{aligned} TC_l &\geq TS1_l \cdot \delta_{ab} - \beta 1_l \\ TC_l &\leq TS2_l \cdot \delta_{ab} + \beta 2_l \\ &\forall l = 1 \; to \; NT, \quad (a, b) \in l \end{aligned} \tag{22}$$

To obtain the value of $\beta 1_l$ and $\beta 2_l$, we focus on finding the angles $\delta 1_{Tl}$ and $\delta 2_{Tl}$ at which lines can be drawn to be tangential to the tangent function within the angle difference range. Starting with $\delta 1_{Tl}$, we introduce the following optimization problem

$$\min \beta 1_l \tag{23}$$

$$TS1_l \cdot \delta 1_{Tl} - \beta 1_l = \tan(\delta 1_{Tl}) \tag{24}$$

$$-|\underline{\delta_l}| \leq \delta 1_{Tl} \leq |\underline{\delta_l}| \tag{25}$$

The aforementioned optimization problem is nonconvex and it also contains equality and inequality constraints. Hence, we use Karush-Kuhn-Tucker (KKT) conditions to solve it [44]. We start solving the problem by writing its Lagrangian equation as follows:

$$\begin{aligned} L = \beta 1_l &+ \lambda \cdot \left(TS1_l \cdot \delta 1_{Tl} - \beta 1_l - \tan\left(\delta 1_{Tl}\right)\right) \\ &+ \mu_1 \left(\delta 1_{Tl} - |\underline{\delta_l}|\right) + \mu_2 \left(-\delta 1_{Tl} - |\underline{\delta_l}|\right) \end{aligned} \tag{26}$$

Since we know that constraint (25) is not binding, the coefficients μ_1 and μ_2 will equal zero. We conclude following differentiating the Lagrangian function with respect to its variables and solving the resulting equations that:

$$\delta 1_{Tl} = sec^{-1}\sqrt{TS1_l} \tag{27}$$

$$\beta 1_l = TS1_l \cdot \delta 1_{Tl} - \tan(\delta 1_{Tl}) \tag{28}$$

Note that (23) – (25) can be used to find $\delta 2_{Tl}$ and $\beta 2_l$ by replacing $TS1_l$ by $TS2_l$. This would result in obtaining $\delta 2_{Tl}$ and $\beta 2_l$ to be:

$$\delta 2_{Tl} = sec^{-1}\sqrt{TS2_l} \tag{29}$$

$$\beta 2_l = TS2_l \cdot \delta 2_{Tl} - \tan(\delta 2_{Tl}) \tag{30}$$

Also, in case when $|\underline{\delta_l}| = |\overline{\delta}_l|$, $TS1_l = TS2_l$, $\delta 1_{Tl} = \delta 2_{Tl}$ and $\beta 1_l = \beta 2_l$. Fig. 2 shows the proposed convex envelopes of the tangent function for different cases where $|\underline{\delta_l}| \neq |\overline{\delta}_l|$ and $|\underline{\delta_l}| = |\overline{\delta}_l|$ where $\underline{\delta_l} < 0, \overline{\delta}_l > 0$.

2) CONVEX ENVELOPE OF THE TANGENT FUNCTION WHERE $\underline{\delta_l} > 0, \overline{\delta}_l > 0$ AND $0 \leq \delta_{ab} \leq \frac{\pi}{2}$

For this case, the tangent function is convex over the angle range. While the convex envelope that was defined for the case where $\underline{\delta_l} < 0, \overline{\delta}_l > 0$ is general in nature and can be applied for this case, the convexity of the tangent function over this angle range allows for utilizing the characteristics of convex functions to tighten the convex envelope. A function is convex over a certain domain if it's value for any point that is within that domain which lies between two points x, y is lower than a line that connects these two points. Mathematically speaking, this can be expressed as

$$f\left(\alpha x + (1-\alpha)\, y\right) \leq \alpha f\left(x\right) + (1-\alpha) f\left(y\right), \quad \forall \alpha \in [0, 1] \tag{31}$$

This implies that for a voltage difference angle range $\underline{\delta_l} \leq \delta_{ab} \leq \overline{\delta}_l$ where $0 \leq \delta_{ab} \leq \frac{\pi}{2}$, a line that connects the points $(\underline{\delta_l}, \tan(\underline{\delta_l}))$ and $(\overline{\delta}_l, \tan(\overline{\delta}_l))$ would provide an upper boundary line for the tangent function envelope. This allows the proposed convex envelope of the tangent function that was defined in (22) to be altered to:

$$\begin{aligned} TC_l &\geq \tan\left(\delta_{ab}\right) \\ TC_l &\leq TSM_l \cdot \delta_{ab} - TSM_l \cdot \underline{\delta_l} + \tan\left(\underline{\delta_l}\right) \\ &\forall l = 1 \; to \; NT, \quad (a, b) \in l \end{aligned} \tag{32}$$

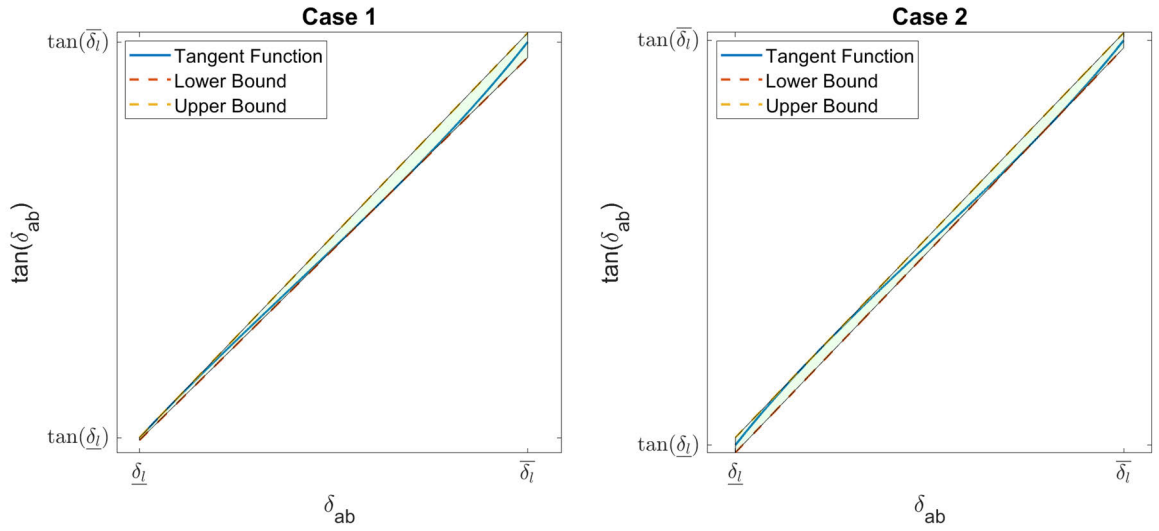

FIGURE 2. Convex envelopes of the tangent function between $\underline{\delta}_l$ and $\overline{\delta}_l$ where $\underline{\delta}_l$ and $\overline{\delta}_l$ are - 20° and + 30° for Case 1, - 30° and + 30° for Case 2.

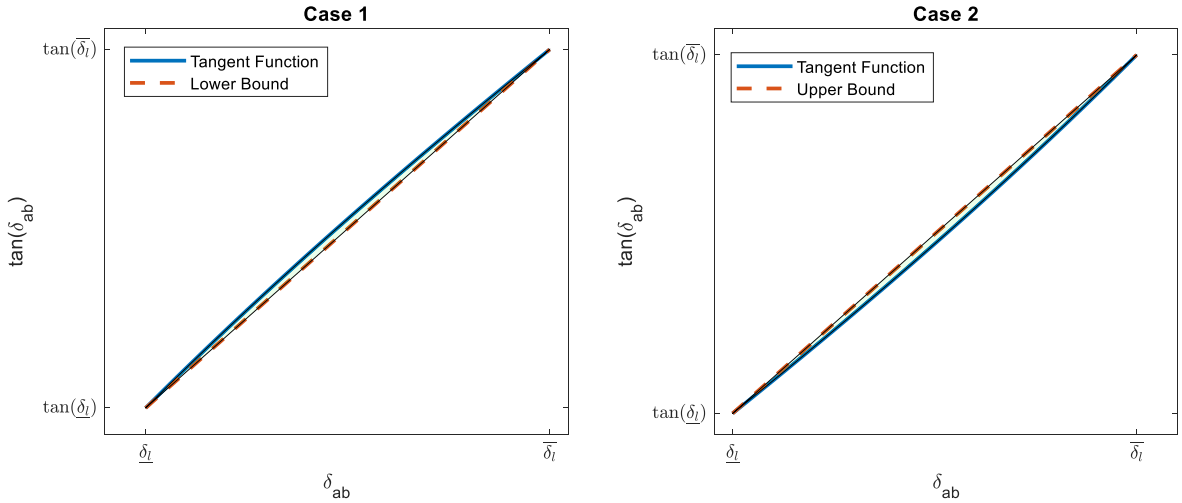

FIGURE 3. Convex envelopes of the tangent function between $\underline{\delta}_l$ and $\overline{\delta}_l$ where $\underline{\delta}_l$ and $\overline{\delta}_l$ are $-30°$ and $-15°$ for Case 1, $+15°$ and $+30°$ for Case 2.

where:

$$TSM_l = \frac{\tan\left(\overline{\delta}_l\right) - \tan(\underline{\delta}_l)}{\overline{\delta}_l - \underline{\delta}_l} \tag{33}$$

3) CONVEX ENVELOPE OF THE TANGENT FUNCTION WHERE $\underline{\delta}_l < 0, \overline{\delta}_l < 0$ AND $-\frac{\pi}{2} \leq \delta_{ab} \leq 0$

Similarly, the fact that the tangent function is concave over this angle range allows the proposed convex envelope of the tangent function that was defined in (22) to be altered to:

$$\begin{aligned} TC_l &\geq TSM_l \cdot \delta_{ab} - TSM_l \cdot \underline{\delta}_l + \tan\left(\underline{\delta}_l\right) \\ TC_l &\leq \tan\left(\delta_{ab}\right) \\ &\forall l = 1 \; to \; NT, \quad (a,b) \in l \end{aligned} \tag{34}$$

Fig. 3 shows the proposed convex envelopes for test cases where $\underline{\delta}_l > 0, \overline{\delta}_l > 0$ and $\underline{\delta}_l < 0, \overline{\delta}_l < 0$ ■

C. COMPLETE CONVEX RELAXATION OF THE LW OPF

The complete nonconvex LW OPF problem (1) – (13) is relaxed and represented in a convex form as below.

- Objective Function (1)

Subject to:

- Bus power balance equations: (6) – (7);
- Limits on Voltage phasor magnitude and angle: (8), (9);
- Limits on active and reactive power generation: (10) – (11);
- Limits on apparent Power Flow in circuits: (12) – (13);
- Relaxation of constraints (2) – (3): (14) – (15);
- Bus voltage magnitude and the squared current Relation to circuit's apparent power flow: (16);
- Relaxation of constraints (4) – (5): (17) – (20);
- Convex envelope of the tangent function: (21) – (22), (27) – (30), (32) – (34);

Additional constraints to enhance the formulation were introduced in [41]. Note that we refer to this formulation as the McCormick based QC relaxation of the LW OPF (QC-LW OPF). The above formulation is a convex nonlinear model of the relaxed LW OPF. It can be solved using a commercial convex optimization solver.

IV. NUMERICAL RESULTS

In this section, we focus on benchmarking the QC-LW OPF against the McCormick based QC relaxation of the BI OPF that is available in the literature where Lifted nonlinear Cuts (LNCs) were used to strengthen it (We refer to this formulation as the QC-BI OPF) [21], [29]. Comparison metrics include Optimality Gap (OG), the recently introduced Cumulative Normalized Constraint Violation (*CNCV*) coefficients [32] and solver computational time. The QC-LW OPF formulation was built in AMPL [45], while the Julia benchmarking library PowerModels.jl was used to obtain the results of the AC-OPF and the QC-BI OPF formulations [46]. The solver IPOPT was used to solve the AC-OPF problem while the solver Gurobi (v 9.1.1) was used to solve the QC-BI OPF and QC-LW OPF problems for all test cases [47], [48]. The Matlab based library MATPOWER was used to obtain power flow results [49]. The IEEE PES PGLib-OPF Task Force library test cases (v21.07) were used in this study [33]. All test cases that belong to three operational categories were considered. However, since Gurobi has not managed to solve the QC-LW OPF and QC-BI OPF for some test cases (due to numerical errors or finding a suboptimal solution), the test cases that were solved to global optimality by Gurobi using the two relaxation schemes are used for comparison. Hence, 39 TYP test cases, 43 API test cases, and 41 SAD test cases (total of 123 test cases) were considered as shown in Table 1. The size range of the considered test cases is between 3 to 6515 buses. Due to the number of considered test cases, box plots are used for conducting statistical analysis of the obtained results. All computational efforts were done using a Thinkpad T480s laptop with CORE i7-8650U CPU and 16 GB of RAM.

TABLE 1. Number of test cases considered per operational category for the numerical experiment.

Operational Category	Number of test cases	Minimum System Size	Maximum System Size
TYP	39	3	6495
API	43	3	6515
SAD	41	3	6515

A. OPTIMALITY GAP

The PES PGLib-OPF Task Force uses the OG metric to evaluate the quality of convex relaxations techniques [33]. Until recently, OG was used extensively in the literature as the sole metric for comparing convex relaxation techniques [32]. OG indicates the distance between the value of the objective functions obtained by solving the OPF problem using a relaxation technique (Lower bound) and the value of the objective functions obtained by solving the OPF problem using a non-convex solver (Higher bound). It is calculated as follows:

$$OG = \frac{Obj^{NC} - Obj^{C}}{Obj^{NC}} \times 100$$

OG was calculated for all test cases that were solved using QC-LWOPF and QC-BIOPF and the results for each operational category are shown in Fig. 4. Furthermore, the 25th, 50th and 75th percentiles for each of the box plots in Fig. 4 are shown in Table 2. Upon examining Fig. 4 and Table 2, we notice that obtained OGs using the QC-BI relaxation and the QC-LW relaxation to solve the OPF problem are very similar numerically. Furthermore, the results show the tendency of both QC relaxations to be affected similarly by the change in the operating conditions with them being the most accurate for the TYP operating conditions and the least accurate for the API operating conditions. Hence, we conclude that both the QC relaxations are equivalent in terms of the value of the OG.

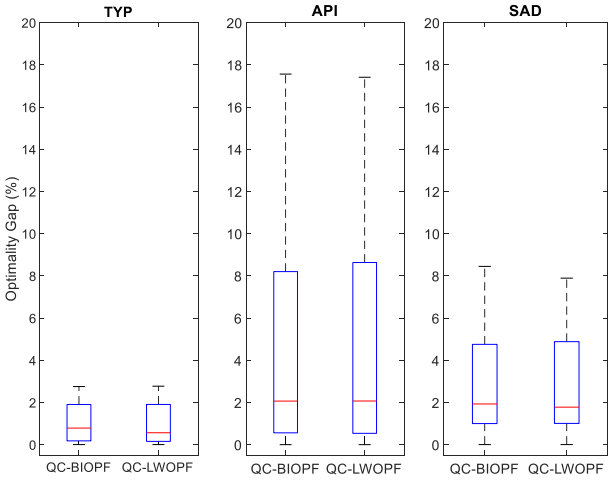

FIGURE 4. Optimality gap for test cases that belong to three operating conditions upon using the enhanced QC-BI and the QC-LW to solve the OPF problem.

TABLE 2. The 25th,50th, and 75th percentiles of the box plots in Fig. 3.

	TYP-OG(%)		API-OG(%)		SAD-OG(%)	
	QC-BI OPF	QC-LW OPF	QC-BI OPF	QC-LW OPF	QC-BI OPF	QC-LW OPF
25%	0.1791	0.1554	0.5597	0.5366	0.9985	1.0068
50%	0.7851	0.5641	2.0644	2.0678	1.928	1.7765
75%	1.9036	1.9053	8.2003	8.6304	4.7527	4.8799

B. CUMULATIVE NORMALIZED CONSTRAINT VIOLATION

Recent literature has shown that the use of the OG as a sole metric for evaluating the quality of a solution that is obtained using a convex relaxation of the original nonconvex problem is insufficient. This is since OG does not provide information

about the distance between state variables and AC feasibility or local optimality [32]. Authors in [32] have addressed these shortcomings by introducing two novel metrics. The first determines the distance of the problem's state variables to AC feasibility and is known as the Cumulative Normalized Constraint Violation (*CNCV*) percentages. The second determines the distances of the obtained solution with respect to known local optimum and is known as the Averaged Normalized Distance to a Local Solution. This paper focuses on the first metric to review its test case solutions obtained using QC-BI OPF and QC-LW OPF. The calculation of the *CNCV* depends on warm-starting an AC Power Flow (AC-PF) with the voltage magnitude and the generator active power profiles obtained from the convex relaxation stage. Solving the warm-started AC-PF, if converged, will yield a solution where all obtained state variables will be examined to test if their values are within the limits of OPF operational constraints. For each state variable $\gamma := \{PG, QG, V_i, \delta_{ab}, Sfm_l, Sto_l\}$, we define *CNCV* to be

$$CNCV_{\gamma} = \sum_{i \in \Omega} \frac{\max(0, \gamma_i^{AC-PF} - \gamma_i^{max}, \gamma_i^{min} - \gamma_i^{AC-PF})}{\gamma_i^{max} - \gamma_i^{min}} \times 100 \tag{35}$$

where $\Omega = \{NG, NG, NB, NT, NT, NT\}$. *CNCV* was calculated for each of the of the state variables. Furthermore, the total *CNCV* for all state variables as well as the percentage of the violated constraints for all test cases were evaluated. All results are presented in Fig. 4, that shows that the study has been conducted for each operational category separately. Logarithmic scale has been used for representing results in Fig. 5. Minimum constraint violation tolerance of 0.1% was used as it was assumed in [32].

1) TYPICAL OPERATING CONDITIONS

For TYP test cases, AC-PF was warm-started using QC-BI OPF and QC-LW OPF solutions for 39 test cases. MATPOWER has managed to converge for 32 test cases using QC-BI OPF results. The divergence of the AC-PF for several French transmission system (RTE) test cases upon using QC-BI OPF results was reported in [32]. However, warm-starting the AC-PF using QC-LW OPF managed to converge for two additional test cases that belong to the French and Polish test cases (Total of 34 test cases). Thus, the comparison was conducted for test cases where AC-PF has managed to converge using both relaxation techniques. Upon examining Fig. 5, inspecting $CNCV_{\delta_{ab}}$ shows that obtained solutions using the warm-started AC-PF did not violate the voltage angle difference constraint. Furthermore, comparing the $CNCV_{V_i}$, $CNCV_{Sfm_l}$, and $CNCV_{Sto_l}$ percentages shows that differences between both relaxation techniques are insignificant. For the $CNCV_{PG}$, it can be noticed that there were no constraint violations for 50% of the tested cases. However, comparing the 75th percentile for $CNCV_{PG}$ shows a slight advantage for the QC-BI OPF based results. Regarding $CNCV_{QG}$, although the 25th percentile is slightly smaller for the QC-BI OPF based results, comparing the 75th percentile for QC-BI OPF and QC-LW OPF based results (5686% and 2055%) shows that QC-LW OPF based results are superior in reducing it by 63%. Upon comparing the $CNCV_{total}$ and percentage of violated constraints, we notice that the differences are insignificant.

2) CONGESTED OPERATING CONDITIONS

For API test cases, warm-started AC-PF studies were conducted for 43 test cases. The AC-PF has converged for 34 test cases when warm-started using QC-BI OPF results. On the other hand, the use of QC-LW OPF results for warm-starting the AC-PF has managed to converge for an additional case (a total of 35 test cases). Hence, 34 test cases were considered for comparing the two QC relaxations. Upon examining Fig. 5, it is noted that the previous observation about the voltage angle difference is valid. Comparing $CNCV_{V_i}$ shows that although both relaxation techniques have managed not to violate the constraint for 25% of tested cases, the comparison of the 50th and 75th percentiles show that the QC-BI OPF based results have voltage magnitude profiles that are closer to AC feasibility for the remaining 75% of test cases. For the $CNCV_{PG}$, the congested nature of the API test cases has led to more constraint violations if compared to the TYP case study results. Both QC relaxations have managed not to violate the active power generation constraint for 25% of tested cases only and they also have similar 50th percentile value. This indicates the differences in distance to AC feasibility for 50% of the tested cases were insignificant. For the remainder of the test cases, the comparison of the 75th percentiles shows that QC-BI OPF active power generation profiles were marginally closer for the remaining test cases. Regarding the $CNCV_{QG}$, the comparison of the 25th, 50th and 75th percentiles for both relaxation techniques show that their profiles for API test cases are closer to AC feasibility when compared to TYP test cases. The comparison also shows that the use of QC-LW OPF has managed to reduce the 50th and 75th percentiles significantly by 73% and 62%, hence, indicating closer distance to AC feasibility. Regarding the $CNCV_{Sfm_l}$ and $CNCV_{Sto_l}$, both relaxation techniques have produced similar ranges of *CNCV* for all the tested cases. It is worth mentioning that apparent power flow violations are the largest contributor to $CNCV_{total}$ for API case study. In contrast, the reactive power generation violations are the largest contributor to $CNCV_{total}$ for TYP and SAD case studies. In terms of comparing $CNCV_{total}$ for both relaxation schemes, the accumulated distance for all state variables towards AC feasibility is similar for both relaxation schemes. However, the comparison of the percentage of violated constraints shows that the QC-LW OPF has managed to slightly violate more constraints when compared to the use of QC-BI OPF.

3) SMALL ANGLE DIFFERENCE CONDITIONS

For SAD test cases, warm-started AC-PF was conducted for 41 test cases. Using the QC-BI OPF results, the AC-PF has

managed to converge for 34 test cases. However, the use of QC-LW OPF results have allowed the AC-PF to converge for an additional two test cases. Hence, the *CNCV* comparison will be conducted for 34 test cases as shown in Fig. 5. Regarding the $CNCV_{V_i}$, we notice that both relaxation schemes managed not to violate the corresponding constraint for 50% of the tested cases. They also have similar $CNCV_{V_i}$ for the remaining test cases that is smaller than those obtained for the TYP and API case studies. However, comparing $CNCV_{\delta_{ab}}$ shows that the voltage angle difference constraint has been violated when relaxation results were used to warm-start the AC-PF. This contrasts with the previous two case studies where no angle difference constraint violations were found. Regarding the $CNCV_{PG}$, we notice that the obtained results showed no constraint violations for 50% of the tested cases. However, the comparison of the 75th percentile shows that the use of QC-LW OPF has reduced the 75th percentile by 50%. For the $CNCV_{QG}$, the use of QC-LW OPF is found to be slightly better than the use the QC-BI OPF relaxation technique. The differences in $CNCV_{Sfm_l}$ and $CNCV_{Sto_l}$ were found to be insignificant. The comparison of the 25th and 75th percentiles of the $CNCV_{total}$ for all state variables shows that the use of the QC-LW OPF has managed to reduce them by 10.2% and 16.2% respectively. Such results indicate that the overall cumulative violations of the QC-LW OPF based AC-PF results are smaller and hence, closer to AC feasibility. The comparison of the percentage of violated constraints also shows a slight advantage for the obtained QC-LW OPF results.

C. COMPUTUTIONAL TIME

The reduction in the needed time by the solver Gurobi to solve the QC-LW OPF with respect to QC-BI OPF for each test case is calculated. Results for each operational category are shown in Fig. 6. Examining Fig. 6 shows that QC-LW OPF has a clear and conclusive advantage over the QC-BI OPF in terms of reducing the solver's needed computational time for more than 84% of all tested cases (Around 89.7% of TYP test cases, 81.4% of API test cases and 82.9% of SAD test cases). The 25th and 75th percentiles (representing half of the test case population) for computational time reduction are found to be around 14% and 49% for TYP test cases, 5% and 42% for API test cases, and 7.7% and 46.23% for SAD test cases. The overall computational time reduction has been found to be between 2% up to 67% depending on the operational category.

V. DISCUSSION

In this section, we discuss the relation of the QC-LW relaxation to other established relaxation techniques in the literature in terms of solution quality. We also discuss the effects of the reduction of decision variables needed to represent trigonometric functions and McCormick envelopes as well as the reduction of McCormick envelopes' complexity upon using the QC relaxation on computational time.

A. QC-LW RELAXATION RELATION TO OTHER CONVEX RELAXATIONS IN TERMS OF SOLUTION QUALITY

It was established in the literature that the McCormick-based QC-BI relaxation dominates the SOC relaxation and it neither dominates nor is dominated by the SDP relaxation in terms of solution quality [21]. These observations have been supported by the recently published literature in which the *CNCV* metric for evaluating the quality of convex relaxations was used to compare the QC-BI and SDP relaxations [32]. Hence, by specifying the relationship between the proposed QC-LW relaxation in [41] and the QC-BI relaxation, we can relate the QC-LW relaxation to other convex relaxations. The comparison of experimental results in section IV shows that both relaxation techniques are equivalent in terms of the OG metric and have their own merits in terms of their solution's distances with respect to AC feasibility. The proposed QC-LW relaxation in [41] managed to allow the AC-PF to converge for additional test cases and it significantly reduced $CNCV_{QG}$ for test cases that belong to all TYP and API operating categories. It was also shown that the QC-LW OPF formulation is more suited for the SAD operating category compared to the QC-BI relaxation. However, the QC-BI relaxation tends to provide slightly smaller $CNCV_{V_i}$ and $CNCV_{PG}$ as well as violate less constraints for test cases that belong to TYP and API operating categories. Based on these results, we claim that QC-LW relaxation neither dominates nor is dominated by the QC-BI relaxation in terms of solution quality. This implies that the proposed QC-LW relaxation in [41] dominates the SOC relaxation and neither dominates nor is dominated by the SDP relaxation.

B. EFFECT OF REDUCING DECISION VARIABLES NEEDED FOR REPRESENTING TRIGONOMETRIC FUNCTIONS AND MCCORMICK ENVELOPES AS WELL AS THE REDUCTION OF McCORMICK ENVELOPES' COMPLEXITY UPON USING QC-LW RELAXATION ON SOLVER'S COMPUTATIONAL TIME

As it was established in the recent literature [41] and supported by the results provided in the previous section, the QC-LW relaxation has a clear advantage in terms of reducing computational time needed by the solver Gurobi to solve the relaxed OPF problem over the QC-BI relaxation. A thorough analysis that has identified the factors which have led to such a performance was provided in [41]. These factors include the ability of the QC-LW OPF formulation to omit the need for McCormick envelopes for convexifying the expression V_a^2. Furthermore, the QC-LW OPF replaces the nonconvex trilinear expression $V_a \cdot V_b \cdot \cos(\delta_{ab})$ by its linear LWM based equivalent (as shown in (20)) which has significantly reduced both the number and complexity of McCormick envelopes needed for the sake of relaxing the expression $V_a \cdot V_b \cdot \cos(\delta_{ab}) \cdot tan(\delta_{ab})$ since it was replaced by the bilinear expression $K_l \cdot TC_l$ (which can be convexified using a single McCormick envelope as shown in (19)). Moreover, the QC-LW OPF formulations reduces the needed number of McCormick envelopes for representing trigonometric func-

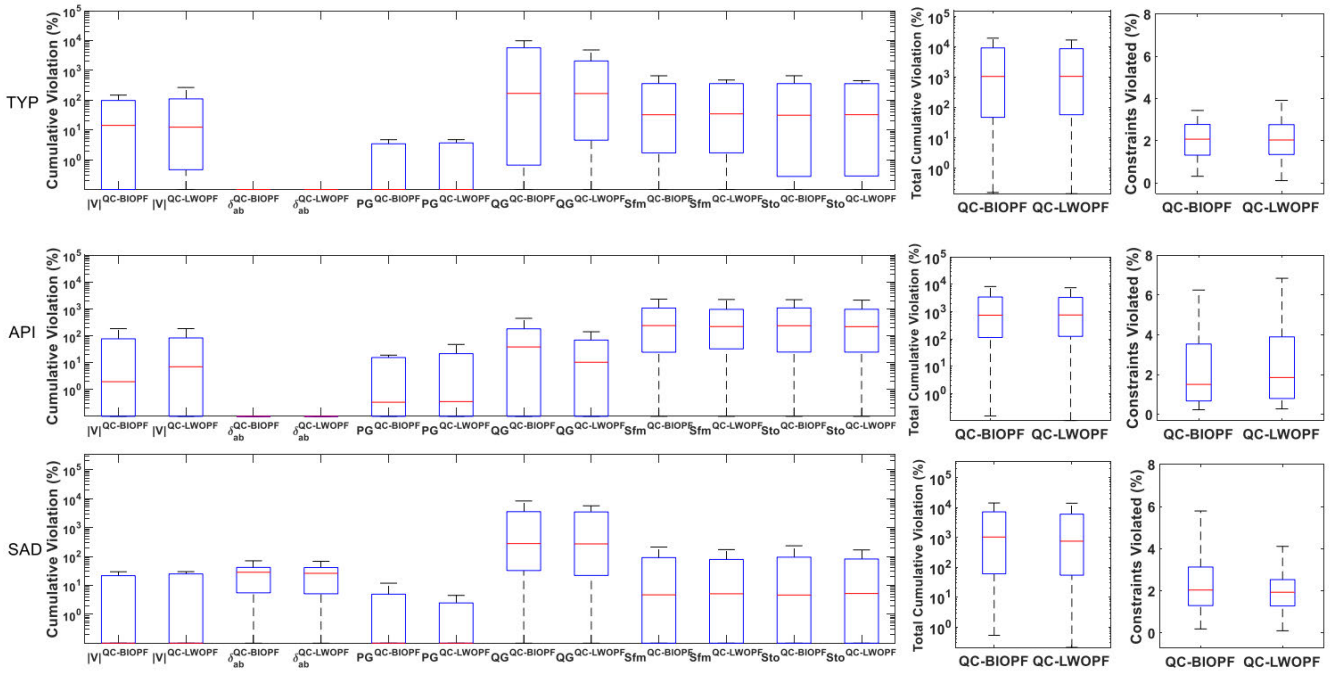

FIGURE 5. Comparison of CNCV calculated for each state variable, CNCV for all state variables and percentage of violated constraints when QC-BI OPF and QC-LW OPF results are used to warm-start AC-PF for three operational categories.

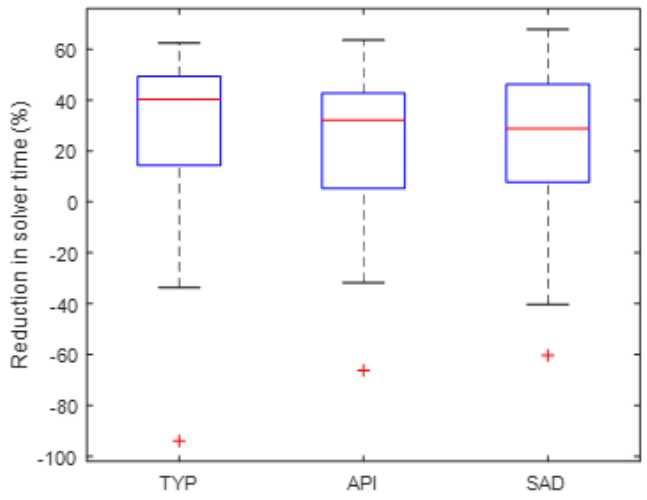

FIGURE 6. Reduction in computational time when QC-LW OPF is used with respect to the use of QC-BI OPF for three operational categories.

TABLE 3. Needed decision variables for convex relaxation of trigonometry functions and McCormick envelopes per relaxed OPF formulation −6515 bus test system.

Relaxation/McCormick Envelope	QC-BI	QC-LW
V_a^2	6,515	0
$V_a \cdot V_B$	9,037	0
$V_a \cdot V_B \cdot \cos(\delta_{ab})$	9,037	0
$V_a \cdot V_B \cdot \sin(\delta_{ab})$	9,037	0
$V_a \cdot V_b \cdot cos(\delta_{ab}) \cdot tan(\delta_{ab})$	0	9,037
$\cos(\delta_{ab})$	9,037	0
$\sin(\delta_{ab})$	9,037	0
$\tan(\delta_{ab})$	0	9,037
Total Number	51,700	18,074

tions due to its dependence on the tangent function (if compared to the QC-BI OPF formulation that depends on both the since and cosine function). Such reductions would have a direct impact on the number of needed decision variables by the QC-LW OPF formulation if compared to the QC-BI OPF formulation.

To illustrate this, we use the 6515-bus test system that has 9037 active lines as an example, we calculate the number of needed decision variables for representing McCormick envelopes and trigonometric functions needed by the QC-BI and QC-LW relaxation techniques. The numbers that are shown in Table 3 state that the use of the QC-LW relaxation has resulted in reducing the needed decision variables required for the relaxed trigonometric functions and McCormick envelopes by 65%. Such a reduction is responsible for enhancing solution space and reducing computational time needed by the solver Gurobi to solve the relaxed QC-LW OPF problem for more than 84% of test cases that belong to the three operating categories when compared to the use of QC-BI relaxation. The literature has established that the QC-BI relaxation is faster and more reliable than the SDP relaxation [21]. This implies that the QC-LW relaxation is more computationally efficient and reliable than the SDP relaxation.

VI. CONCLUSION

In this paper, a computational study where the recently proposed McCormick-based QC-LW OPF formulation in the literature [41] has been tested for solving the OPF problem is provided. This study -unlike the limited results that were provided in [41]- was carried on a larger set of test cases that belong to different operating conditions with a wider bus size range (A total of 123 test systems taken from the IEEE PES PGLib-OPF Task Force library with bus sizes of 3 up to 6515 buses were considered). This study's intention is to decisively determine the relationship between the QC-LW OPF formulation and other relevant convex relaxations in the literature in terms of solution's quality and computational complexity. Furthermore, this study has examined the effect of the operating conditions of the considered test cases on the quality of the obtained solutions using the QC-LW OPF formulation by conducting the experiment for test cases that belong to each of the three operational categories separately. The paper has also extended the proposed convex envelope of the tangent function in [41] so it would be suitable for test cases with symmetrical and asymmetrical angle ranges. The recently introduced McCormick-based QC-LW relaxation was compared to the established McCormick-based QC-BI relaxation in the literature.

Analysing the results of OG and *CNCV* percentages obtained for the test cases that belong to the three operating categories shows that in terms of solution quality, the recently introduced QC-LW relaxation neither dominates nor is dominated by the QC-BI relaxation and hence, it dominates the SOC relaxation and neither dominates nor is dominated by the SDP relaxation.

Moreover, the paper finds that the recently introduced QC-LW OPF manages to provide a faster and more reliable solver performance for more than 84% of test cases in comparison with the QC-BI OPF results where computational time reductions were in the range of 2% to 67% depending on the operational category. Such improvements in solver performance are attributed to the significant reductions in the number of needed decision variables to represent convex envelopes of trigonometric functions and McCormick envelopes as well as the reduction in complexity of McCormick envelopes that were used to relax the OPF problem using the recently introduced QC-LW relaxation. The establishment of the QC-LW relaxation to be more computationally efficient than the QC-BI relaxation implies its dominance over the SDP relaxation in terms of solver computational time and reliability. The merits of the recently introduced QC-LW relaxation may encourage the power systems community to pay closer attention to the LWM for modeling power systems for different power system studies where convex relaxation is needed. Future directions include applying enhancements reported in [50] and [51] to strengthen the QC-BI Relaxation to the QC-LW relaxation.

REFERENCES

[1] J. A. Taylor. (Feb. 2015). *Convex Optimization of Power Systems*. Cambridge Core. Accessed: Aug. 1, 2019. [Online]. Available: https://www.cambridge.org/core/books/convex-optimization-of-power-systems/4CCA9CC35F35AE7EB222B07F2AD7FA98

[2] J. Carpentier, "Contribution a l'etude du dispatching economique," *Bull. de la Societe Francaise des Electriciens*, vol. 3, pp. 431–447, Aug. 1962.

[3] M. B. Cain, R. P. O'Neill, and A. Castillo, "History of optimal power flow and formulations: Optimal power flow paper 1," US FERC, Washington, DC, USA, Tech. Rep., 36, Dec. 2012.

[4] I. A. Hiskens and R. J. Davy, "Exploring the power flow solution space boundary," *IEEE Trans. Power Syst.*, vol. 16, no. 3, pp. 389–395, Aug. 2001, doi: 10.1109/59.932273.

[5] H. W. Dommel and W. F. Tinney, "Optimal power flow solutions," *IEEE Trans. Power App. Syst.*, vol. PAS-87, no. 10, pp. 1866–1876, Oct. 1968, doi: 10.1109/TPAS.1968.292150.

[6] O. Alsac and B. Stott, "Optimal load flow with steady-state security," *IEEE Trans. Power App. Syst.*, vol. PAS-93, no. 3, pp. 745–751, May 1974, doi: 10.1109/TPAS.1974.293972.

[7] R. C. Burchett, H. H. Happ, and K. A. Wirgau, "Large scale optimal power flow," *IEEE Trans. Power App. Syst.*, vol. PAS-101, no. 10, pp. 3722–3732, Oct. 1982, doi: 10.1109/TPAS.1982.317057.

[8] R. C. Burchett, H. H. Happ, and D. R. Vierath, "Quadratically convergent optimal power flow," *IEEE Trans. Power App. Syst.*, vol. PAS-103, no. 11, pp. 3267–3275, Nov. 1984, doi: 10.1109/TPAS.1984.318568.

[9] J. A. Momoh, "A generalized quadratic-based model for optimal power flow," in *Proc. IEEE Int. Conf. Syst., Man Cybern.*, Nov. 1989, pp. 261–271, doi: 10.1109/ICSMC.1989.71294.

[10] M. A. Abido, "Optimal power flow using particle swarm optimization," *Int. J. Elect. Power Energy Syst.*, vol. 24, no. 7, pp. 563–571, 2002, doi: 10.1016/S0142-0615(01)00067-9.

[11] A. G. Bakirtzis, P. N. Biskas, C. E. Zoumas, and V. Petridis, "Optimal power flow by enhanced genetic algorithm," *IEEE Trans. Power Syst.*, vol. 18, no. 3, pp. 1219–1220, Aug. 2003, doi: 10.1109/TPWRS.2002.807109.

[12] A. A. Mohamed and B. Venkatesh, "Line-wise optimal power flow using successive linear optimization technique," *IEEE Trans. Power Syst.*, vol. 34, no. 3, pp. 2083–2092, May 2019, doi: 10.1109/TPWRS.2018.2881254.

[13] S. Bolognani and F. Dorfler, "Fast power system analysis via implicit linearization of the power flow manifold," in *Proc. 53rd Annu. Allerton Conf. Commun., Control, Comput. (Allerton)*, Sep. 2015, pp. 402–409, doi: 10.1109/ALLERTON.2015.7447032.

[14] D. Deka, S. Backhaus, and M. Chertkov, "Structure learning and statistical estimation in distribution networks—Part I," 2015, *arXiv:1501.04131*.

[15] J. Yang, N. Zhang, C. Kang, and Q. Xia, "A state-independent linear power flow model with accurate estimation of voltage magnitude," *IEEE Trans. Power Syst.*, vol. 32, no. 5, pp. 3607–3617, Sep. 2017, doi: 10.1109/TPWRS.2016.2638923.

[16] F. Capitanescu, "Critical review of recent advances and further developments needed in AC optimal power flow," *Electric Power Syst. Res.*, vol. 136, pp. 57–68, Jul. 2016, doi: 10.1016/j.epsr.2016.02.008.

[17] S. Frank and S. Rebennack, "An introduction to optimal power flow: Theory, formulation, and examples," *IIE Trans.*, vol. 48, no. 12, pp. 1172–1197, Aug. 2016. [Online]. Available: https://www.tandfonline.com/doi/abs/10.1080/0740817X.2016.1189626

[18] H. Abdi, S. D. Beigvand, and M. La Scala, "A review of optimal power flow studies applied to smart grids and microgrids," *Renew. Sustain. Energy Rev.*, vol. 71, pp. 742–766, May 2017, doi: 10.1016/j.rser.2016.12.102.

[19] R. A. Jabr, "Radial distribution load flow using conic programming," *IEEE Trans. Power Syst.*, vol. 21, no. 3, pp. 1458–1459, Aug. 2006, doi: 10.1109/TPWRS.2006.879234.

[20] X. Bai, H. Wei, K. Fujisawa, and Y. Wang, "Semidefinite programming for optimal power flow problems," *Elect. Power Energy Syst.*, vol. 30, no. 6, pp. 383–392, Dec. 2008, doi: 10.1016/j.ijepes.2007.12.003.

[21] C. Coffrin, H. L. Hijazi, and P. Van Hentenryck, "The QC relaxation: A theoretical and computational study on optimal power flow," *IEEE Trans. Power Syst.*, vol. 31, no. 4, pp. 3008–3018, Jul. 2016, doi: 10.1109/TPWRS.2015.2463111.

[22] M. Farivar and S. H. Low, "Branch flow model: Relaxations and convexification—Part II," *IEEE Trans. Power Syst.*, vol. 28, no. 3, pp. 2565–2572, Aug. 2013, doi: 10.1109/TPWRS.2013.2255318.
[23] S. H. Low, "Convex relaxation of optimal power flow—Part I: Formulations and equivalence," *IEEE Trans. Control Netw. Syst.*, vol. 1, no. 1, pp. 15–27, Mar. 2014, doi: 10.1109/TCNS.2014.2309732.
[24] S. H. Low, "Convex relaxation of optimal power flow—Part II: Exactness," *IEEE Trans. Control Netw. Syst.*, vol. 1, no. 2, pp. 177–189, Jun. 2014, doi: 10.1109/TCNS.2014.2323634.
[25] J. Lavaei and S. H. Low, "Zero duality gap in optimal power flow problem," *IEEE Trans. Power Syst.*, vol. 27, no. 1, pp. 92–107, Feb. 2012, doi: 10.1109/TPWRS.2011.2160974.
[26] B. C. Lesieutre, D. K. Molzahn, A. R. Borden, and C. L. DeMarco, "Examining the limits of the application of semidefinite programming to power flow problems," in *Proc. 49th Annu. Allerton Conf. Commun., Control, Comput. (Allerton)*, Sep. 2011, pp. 1492–1499, doi: 10.1109/Allerton.2011.6120344.
[27] H. Hijazi, C. Coffrin, and P. V. Hentenryck, "Convex quadratic relaxations for mixed-integer nonlinear programs in power systems," *Math. Program. Comput.*, vol. 9, no. 3, pp. 321–367, Sep. 2017, doi: 10.1007/s12532-016-0112-z.
[28] G. P. McCormick, "Computability of global solutions to factorable nonconvex programs: Part I—Convex underestimating problems," *Math. Program.*, vol. 10, no. 1, pp. 147–175, Dec. 1976, doi: 10.1007/BF01580665.
[29] C. Coffrin, H. L. Hijazi, and P. Van Hentenryck, "Strengthening the SDP relaxation of AC power flows with convex envelopes, bound tightening, and valid inequalities," *IEEE Trans. Power Syst.*, vol. 32, no. 5, pp. 3549–3558, Sep. 2017, doi: 10.1109/TPWRS.2016.2634586.
[30] D. K. Molzahn and I. A. Hiskens, *A Survey of Relaxations and Approximations of the Power Flow Equations*. The Netherlands: Now. Accessed: Oct. 16, 2019. [Online]. Available: https://ieeexplore.ieee.org/document/8635446 and https://www.nowpublishers.com/Home/Contact
[31] F. Zohrizadeh, C. Josz, M. Jin, R. Madani, J. Lavaei, and S. Sojoudi, "A survey on conic relaxations of optimal power flow problem," *Eur. J. Oper. Res.*, vol. 287, no. 2, pp. 391–409, Dec. 2020, doi: 10.1016/j.ejor.2020.01.034.
[32] A. Venzke, S. Chatzivasileiadis, and D. K. Molzahn, "Inexact convex relaxations for AC optimal power flow: Towards AC feasibility," *Electric Power Syst. Res.*, vol. 187, Oct. 2020, Art. no. 106480, doi: 10.1016/j.epsr.2020.106480.
[33] S. Babaeinejadsarookolaee, A. Birchfield, R. D. Christie, C. Coffrin, C. DeMarco, R. Diao, M. Ferris, S. Fliscounakis, S. Greene, R. Huang, and C. Josz, "The power grid library for benchmarking AC optimal power flow algorithms," 2019, *arXiv:1908.02788*.
[34] S. Huang, Q. Wu, J. Wang, and H. U. Zhao, "A sufficient condition on convex relaxation of AC optimal power flow in distribution networks," *IEEE Trans. Power Syst.*, vol. 32, no. 2, pp. 1359–1368, Jun. 2017, doi: 10.1109/TPWRS.2016.2574805.
[35] B. Park, M. C. Ferris, and C. L. DeMarco, "Benefits of sparse tableau over nodal admittance formulation for power-flow studies," *IEEE Trans. Power Syst.*, vol. 34, no. 6, pp. 5023–5032, Nov. 2019, doi: 10.1109/TPWRS.2019.2916719.
[36] B. Park and C. L. DeMarco, "Convex relaxation of sparse tableau formulation for the AC optimal power flow," *Electr. Power Syst. Res.*, vol. 171, pp. 209–218, Jun. 2019, doi: 10.1016/j.epsr.2019.02.020.
[37] A. A. Mohamed and B. Venkatesh, "Line-wise power flow and voltage collapse," *IEEE Trans. Power Syst.*, vol. 33, no. 4, pp. 3768–3778, Jul. 2018, doi: 10.1109/TPWRS.2017.2787752.
[38] A. A. Mohamed and B. Venkatesh, "Voltage stability constrained line-wise optimal power flow," *IET Gener. Transmiss. Distrib.*, vol. 13, no. 8, pp. 1332–1338, 2019, doi: 10.1049/iet-gtd.2018.5452.
[39] A. A. Mohamed and B. Venkatesh, "Linearized voltage stability incorporation with line-wise optimal power flow," *Int. J. Electr. Power Energy Syst.*, vol. 108, pp. 232–239, Jun. 2019, doi: 10.1016/j.ijepes.2019.01.005.
[40] A. Aldik and B. Venkatesh, "Reactive power planning using convex line-wise power balance equations for radial distribution systems," *IET Gener., Transmiss. Distrib.*, vol. 14, no. 12, pp. 2399–2406, Feb. 2020, doi: 10.1049/iet-gtd.2019.1841.
[41] A. R. Aldik and B. Venkatesh, "AC transmission network expansion planning using the line-wise model for representing meshed transmission networks," *IEEE Trans. Power Syst.*, early access, Jun. 16, 2022, doi: 10.1109/TPWRS.2022.3183549.
[42] A. R. Aldik and B. Venkatesh, "Fast SDP relaxation of the optimal power flow using the line-wise model for representing meshed transmission networks," *IEEE Trans. Power Syst.*, early access, Aug. 23, 2022, doi: 10.1109/TPWRS.2022.3200970.
[43] *Tangent Function—Calculus*. Accessed: Jul. 28, 2022. [Online]. Available: https://calculus.subwiki.org/wiki/Tangent_function#Intervals_of_concave_up_and_concave_down
[44] S. I. Gass and M. C. Fu, "Karush–Kuhn–Tucker (KKT) conditions," in *Encyclopedia of Operations Research and Management Science*. Boston, MA, USA: Springer, 2013, pp. 833–834, doi: 10.1007/978-1-4419-1153-7_200359.
[45] R. Fourer, D. M. Gay, and B. W. Kernighan, "AMPL: A mathematical programming language," *Manag. Sci.*, vol. 36, pp. 519–554, Jan. 1989.
[46] C. Coffrin, R. Bent, K. Sundar, Y. Ng, and M. Lubin, "PowerModels.Jl: An open-source framework for exploring power flow formulations," 2017, *arXiv:1711.01728*.
[47] A. Wächter and L. T. Biegler, "On the implementation of an interior-point filter line-search algorithm for large-scale nonlinear programming," *Math. Program.*, vol. 106, no. 1, pp. 25–57, May 2006, doi: 10.1007/s10107-004-0559-y.
[48] *Gurobi Optimizer Reference Manual*, Gurobi Optimization, LLC, USA, 2020, p. 969. [Online]. Available: https://www.gurobi.com/company/contact-us/
[49] R. D. Zimmerman, C. E. Murillo-Sánchez, and R. J. Thomas, "MATPOWER: Steady-state operations, planning, and analysis tools for power systems research and education," *IEEE Trans. Power Syst.*, vol. 26, no. 1, pp. 12–19, Feb. 2011, doi: 10.1109/TPWRS.2010.2051168.
[50] K. Sundar, H. Nagarajan, S. Misra, M. Lu, C. Coffrin, and R. Bent, "Optimization-based bound tightening using a strengthened QC-relaxation of the optimal power flow problem," 2018, *arXiv:1809.04565*.
[51] M. R. Narimani, D. K. Molzahn, and M. L. Crow, "Tightening QC relaxations of AC optimal power flow problems via complex per unit normalization," *IEEE Trans. Power Syst.*, vol. 36, no. 1, pp. 281–291, Jan. 2021, doi: 10.1109/TPWRS.2020.3004289.

ABDEL RAHMAN ALDIK (Member, IEEE) received the B.Sc. degree in electrical engineering from An-Najah National University, Nablus, Palestine, in 2010, and the M.Sc. degree in electrical engineering from the King Fahd University of Petroleum and Minerals (KFUPM), Dhahran, Saudi Arabia, in 2015. He is currently pursuing the Ph.D. degree with Toronto Metropolitan University, Toronto, ON, Canada. Then, he joined the Department of Electrical, Computer and Biomedical Engineering, Toronto Metropolitan University, as a Research Assistant, in 2018. He joined An-Najah National University, as a Research Assistant, in 2011, and he worked with Palestinian Telecommunications Company (PALTEL), until 2012. He rejoined An-Najah National University, as a Lecturer, in 2015. His research interests include power system planning, operations, and power system optimization.

BALA VENKATESH (Senior Member, IEEE) received the Ph.D. degree from Anna University, India, in 2000. He is currently a Professor and an Academic Director of the Centre for Urban Energy, Toronto Metropolitan University, Toronto, Canada. His research interests include power system analysis and optimization. He is a Registered Professional Engineer in the province of Ontario, Canada.